STRUCTURAL HEALTH MONITORING FOR CONCENTRATED SOLAR PLANTS

Carlos Quiterio Gómez Muñoz, Juan Ramón Trapero Arenas, Fausto Pedro García Márquez

Ingenium Research Group,
Universidad de Castilla-La Mancha
Ciudad Real, Edificio Politécnica 13071, Spain
carlosquiterio.gomez@gmail.com

Abstract

Renewable energy is being one of the options to cover the demand due to the environmental restrictions. One of the most relevant renewable energy sources is the solar energy, where the concentrated solar power is nowadays the source that is getting more importance. The correct performance of solar receiver is crucial because its failure can result in significant costs and availability of the energy service. Non-destructive testing is broadly used in structural health monitoring systems in order to detect and diagnose faults/failures.
The aim of this paper is to present a fault detection and diagnosis approach based on long range ultrasonic technology, together with novel analytical procedures on signal processing of high frequency waves (Lamb waves). These waves flow through the material via the piezoelectric transducers, where these transducers are also employed as sensors. The fault can be detected and diagnosed by changes in the signal when it is modified by the fault. The experimental platform consists of: i) a data logger able to generate and read voltage signals at high frequency; ii) a sensing system based on piezoelectric transducers placed at the solar collector. A novel method of analyzing the data generated in the platform by means of time series is employed.

1. Introduction

Non-destructive testing (NDT) for fault detection in structures have gained relevant attention in recent years due to significant advances in instrumentation technology and digital signal processing. Techniques for Structural Health Monitoring (SHM) permit to identify and diagnose the fault and its location on the basis of changes in static and dynamic structure features. In addition, these techniques can be remotely controlled and they may work online saving important costs associated to manual inspections and warning times. The capability of NDT to prevent faults is one of their main advantages, which typically achieve a better reliability, availability, maintainability and a cost reduction of the system.

Within the NDT field, guided waves are a common technique employed for SHM. These waves are particularly useful in geometries such plates or tubes. This technology is based on the excitation of low frequency ultrasonic waves flowing along the pipeline over long distances and allowing inspections of large areas without any relocation of the actuator, as it occurs in classical ultrasonic methods[(1)]. This technology may be used in pipelines under working conditions and it can be inspected from a single position, what is particularly indicated when monitoring inaccessible areas, e.g. isolated materials, partially buried structures, corrosive atmospheres or structures under the sea[(2)]. Since these signals can be recorded and processed, novel methodologies are arising so as to perform predictive analysis in real time.

The purpose of this paper is to design a Fault Detection and Diagnosis (FDD) model using ultrasound inputs in conjunction with advanced signal processing methods to monitor the structural assessment of Parabolic Trough Receivers (PTR) associated to Concentrated Solar Power (CSP) plants. Note that this study is crucial since the cost of PTR can reach the 30% of the overall solar field cost. Therefore, the correct maintenance of the receivers is of paramount importance to assure that CSP plants work properly. It should be pointed out that, despite the importance of the PTR, its failure rate has been very high. Initially (years 1997-2001) the average annual PTR replacement rate was about 5.5% [(3)]. Nowadays, it has been reduced to 3.37 % [(4)] and forecasts indicate that the replacement rates should decrease up to 0.5 % for a near future [(3)].

The system proposed will be able to detect faults or structural modifications e.g. scratches, cuts, changes in thickness or edges by identifying pattern changes in the input-ouput signals. Note that pattern changes are associated to the aforementioned potential faults. The signal processing is based on system identification techniques in discrete time to estimate potential faults. Particularly, AutoRegressive eXogenous (ARX) models will be employed to identify the structure in fault-free conditions. In case that the solar collector suffers from a fault, the identified model could provide an alarm given the errors between the measurements and the model predicted output. An experimental platform that comprises a data logger able to generate and read voltage signals at high frequency; and a sensing system based on piezoelectric transducers placed at the solar collector is designed in order to illustrate the results.

The article is organized as follows: Section 2 describes the experimental platform. Section 3 explains the procedure to detect defects. Experimental results are detailed in Section 4 and finally, the main conclusions are drawn in Section 5.

2. Experimental platform

Different experiments were carried out in an experimental platform to obtain the proposed FDD. The platform (see Figure 1) consists of a device that is able to read and generate signals up to 4 MS/s. The device is connected to a PC for condition monitoring. The output signal from the device goes through an amplifier to drive the piezoelectric transducers. The high frequency amplifier is used to enhance the signal to noise ratio. Since the actuator is driven by the computer, different input signals can be generated as it will be shown later on.

The piezoelectric transducers used are macro-fiber composites (MFC) working as actuators and sensors. This type of elements has been successfully employed in wind turbine condition monitoring [7-8]

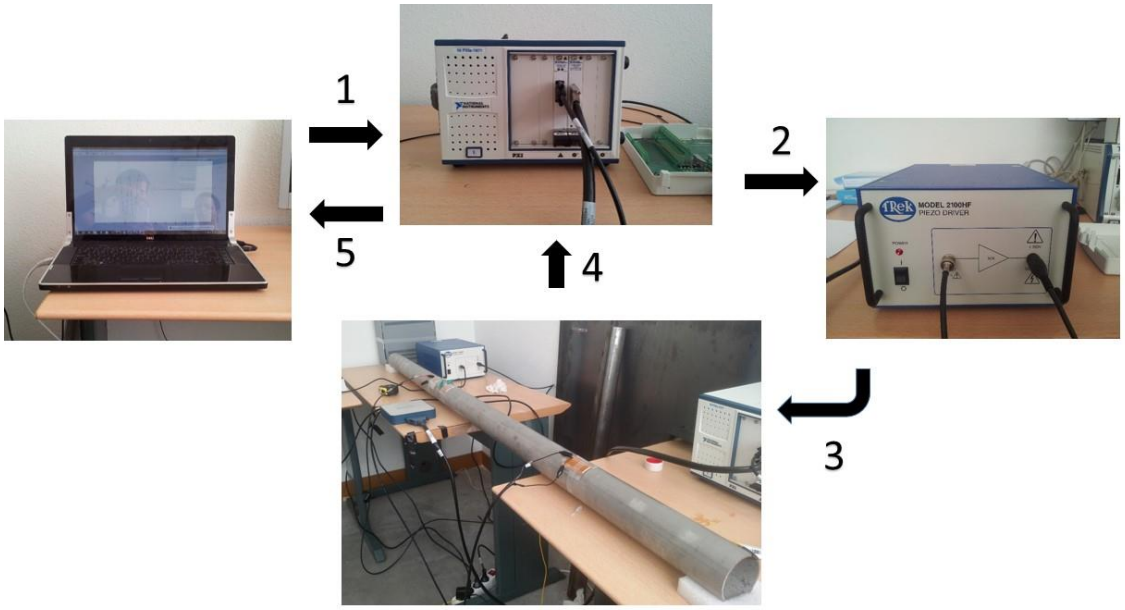

Figure 1. Laboratory NDT.

The experiment procedure can be summarized as follows: an input signal is generated from the computer and sent to the MFC. Such a signal flows through the structure to be inspected and it is read by other MFCs. This technique is called transmission method [6]. If there is a defect e.g. a crack in the transmission direction of the wave, a reflection of part of the wave is received, and therefore, the delay in the wave transmission will be reduced and the piezoelectric sensor will detect that imperfection. Note that this experiment employs three MFCs, where one MFC acts as an actuator and the other two as sensors. The reason of using this layout is to simulate the PTRs in the solar field, in the sense that, one actuator would be located at one extreme of the PTRs serially connected and the rest of sensors would be placed around the PTRs welds, since it is the only area where the tube steel is available.

Figure 2 depicts the layout of the actuator on the left part of the tube and the two sensors (sensor 1 and sensor 2). The main properties of the tube used as a test-bed is also shown in Table 1. Note that the steel employed is the same that the one incorporated in the PTRs.

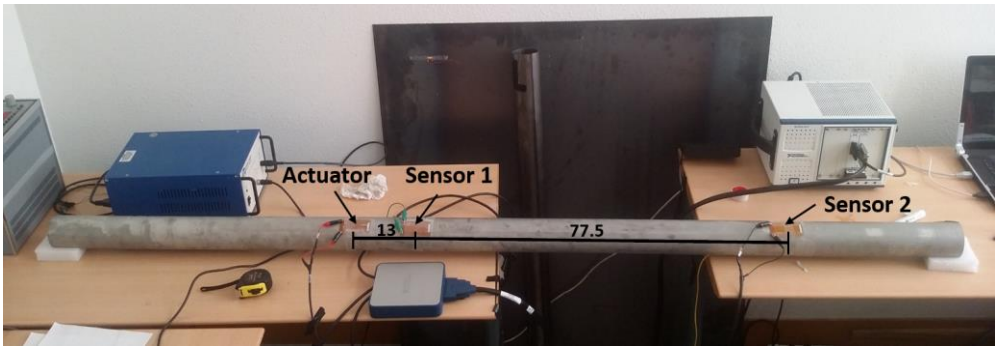

Figure 2. Actuator and sensors placement.

Table 1. Steel properties

Type of steel	Austenitic stainless steel
Nomenclature	316l (AISI) 1.4404 (DIN)
Length	2m
Diameter	73mm
Thickness	3.05mm
Density	7.9 kg/dm^3
Thermal Conductivity	15 W/m.K
Average thermal expansion coefficient	16e10^{-6}
Electrical resistivity	0.75 Ω mm2/m
Magnetic permeability	1.005 a 0.8 kA/m DC or AC
Young longitudinal elastic modulus	200*10e3 MPa
Poisson coefficient	0.3

3. Methodology

In order to detect potential faults, it is necessary to monitory a key variable, where changes of that variable are associated to a high fault probability. The procedure employed to detect such faults is described as follows:

3.1 Selection of pulse frequency

The inputs chosen to excite the system are white noise and Hanning pulses. The idea behind is to use white noise to excite the whole frequency bandwidth to investigate empirically which frequencies are better suited to carry out ultrasound tests. Here, a periodogram[(5)] of the resulting signals will be computed to determine which frequencies present resonant effects. It should be considered that piezoelectric sensors have a high frequency limit, whose response is not reliable for frequencies that exceed that bound.

Therefore, once the working frequency has been chosen, the following experiments based on pulses will be set on the aforementioned frequency. Moreover, it is important to compute the dispersion curves to determine how many vibration modes are to be expected, as well as, their different associated group velocities.

3.2 Delay estimation

The delay between signals will be estimated by means of ARX models. Time series methods have been previously employed to failure prediction and detection. For

instance, a VARMA [9] (vector auto-regressive moving-average) and harmonic regressions [10] have been employed, respectively, to failure prediction in railway elements. Here, an ARX model is proposed to identify faults in solar collectors. Basically, an ARX models can be expressed by a linear difference equation, such as:

$$y_t + a_1 y_1 + \cdots + a_{na} y_{t-na} = b_1 u_{t-nk} + \cdots + b_{nb} u_{t-nk-nb+1} + \varepsilon_t \quad \text{.....(1)}$$

where AR refers to the autoregressive part and X to the extra input, sometimes called the exogenous variable. The parameters n_a and n_b are the orders of the ARX model, and n_k is the number of input samples that occur before the input affects the output, also called the delay in the system [11]. The variables y_t and u_t stand for the output and input responses, respectively. Model orders n_a, n_b and n_k have been chosen by minimizing the Akaike's Information Criterion (AIC) [13], i.e.:

$$AIC = 2k - 2\ln(L) \quad \text{.....(2)}$$

where k is the number of parameters in the statistical model, and L is the maximized value of the likelihood function for the estimated model. The AIC includes a penalty for over fitting as a consequence of incorporating more parameters to the model in (1). To reduce the search space for potential orders (n_a, n_b and n_k) a cross-correlation [5] graph will be used, where the dimensionless cross-correlation coefficient at lag k is given by:

$$\rho_{xy}(k) = \frac{\gamma_{xy}(k)}{\sigma_x \sigma_y}, k = 0, \pm 1, \pm 2, \quad \text{.....(3)}$$

Where γ_{xy} is the cross-covariance between the signal x and the signal y for $k = 0, \pm 1, \pm 2, \ldots$ and σ_x is the standard deviation of signal x.

Model selection and the estimation of the unknown parameters a_i, $i=1,\ldots,n_a$ and b_j, $j=1,\ldots,n_b$ have been done by means of the routines implemented in the MATLAB™ System Identification toolbox [14].

4. Experimental results

According to the procedure previously described. The first step is to excite the system depicted in Figure 2 with a white noise input. Figure 3 depicts the periodogram of the signal measured by sensor 1. In that figure, it can be seen that the frequency that provides a maximum peak is around 30 KHz.

The emitted signal will be a Hanning pulse at 30 kHz, 2 cycles and a sampling frequency of 400,000 samples per second. Recall that the input frequency is set to 30 kHz to achieve a compromise between good response and MFC limitations when they work as actuators. Additionally, the pulse is composed of two cycles to create a narrow pulse and to avoid undesired overlaps between the emitted pulse and the first received echoes. Figure 4 shows the input signal (upper panel), the sensor 1 received signal (middle panel), and the sensor 2 measurements (lower panel). This picture shows clearly

the delay between the input and both sensors. Since sensor 2 is located at a longer distance from the actuator the delay is also bigger.

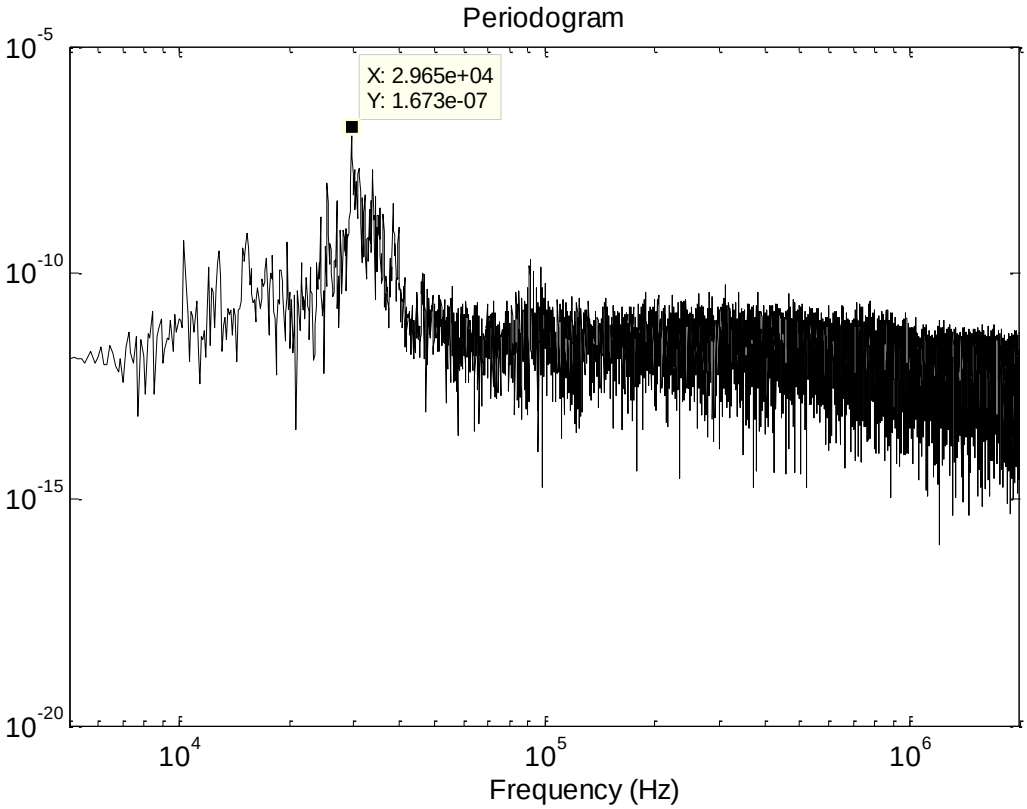

Figure 3. Periodogram of the sensor 1 signal measurements.

According to the previous section, the next step is to identify an ARX model between sensor 1 and sensor 2. To do that, we have to set the ARX model orders. It should be noted that the potential orders of the ARX model depend on the sample time. For instance, when the sample time decreases, the delay represented by n_k in equation (1) increases. In our particular case, since the sampling period is $2.5*10^{-6}$ seconds (1/400,000 samples per second) and the delay should be around $0.2*10^{-3}$ and $0.35*10^{-3}$ seconds by inspecting the lower panel in Figure 4, the delay order n_k should be around 80 ($0.2*10^{-3}$ /$2.5*10^{-6}$) and 140 ($0.35*10^{-3}$ /$2.5*10^{-6}$) lags. Another useful graph to identify the delay order is the sample cross-correlation graph. Figure 5 shows that the maximum cross-correlation coefficient should be between 80 and 140 lags, as it was deducted previously. Bearing in mind that information, the expected order values for the ARX model can be selected by minimizing the AIC criterion for delays ranging from 80 to 140 lags.

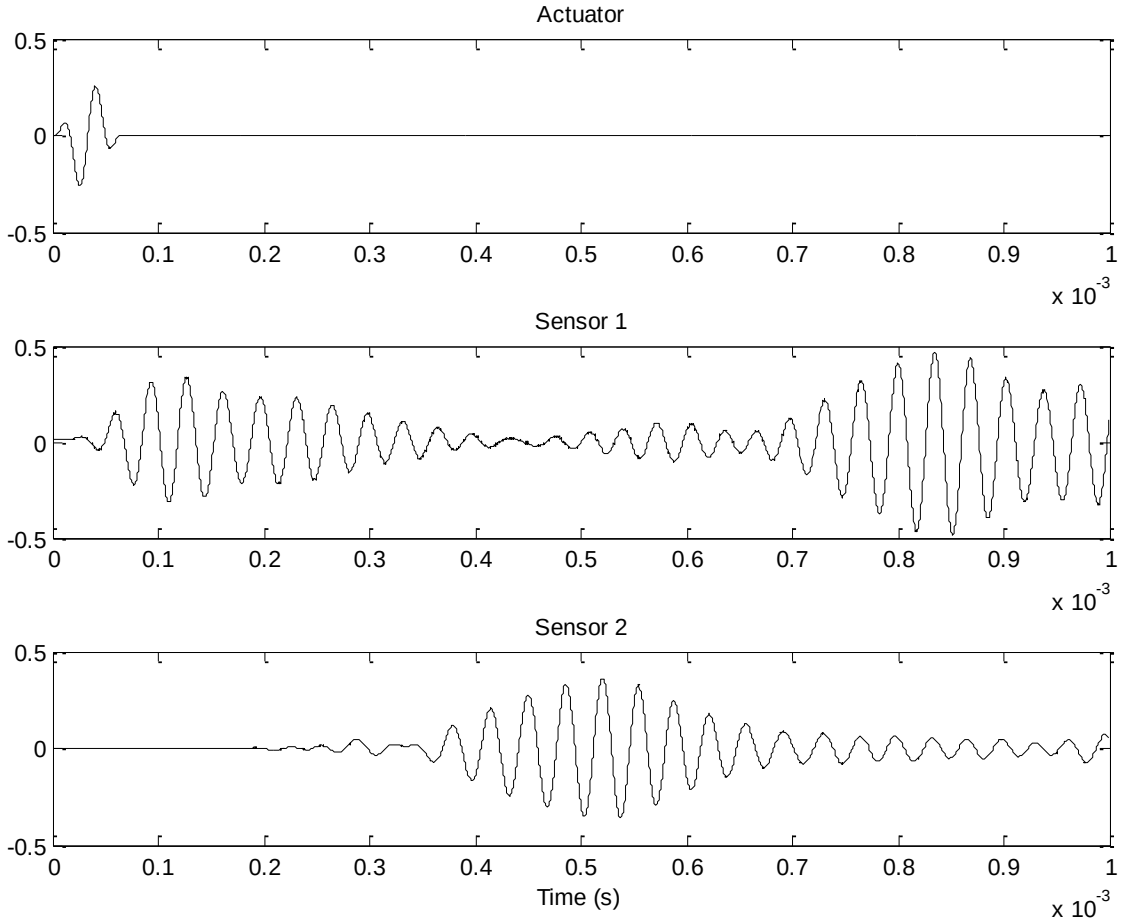

Figure 4. Actuator pulse input (upper panel). Sensor 1 measurements (middle panel). Sensor 2 measurements (lower panel).

The estimated ARX model is:

$$(1 - 1.764z^{-1} + 0.9685z^{-2})y_t = 0.2604z^{-100}u_t + \varepsilon_t \quad \text{.....(4)}$$

Where z is the Z operator, such as: $z^{-1}y_t = y_{t-1}$. Thus, the delay is $n_k * T_s = 100 * 2.5 * 10^{-6} = 2.5 * 10^{-4}$ seconds. In order to corroborate the results, the distance between sensors can be estimated. For instance, considering the delay ($2.5 * 10^{-4}$ seconds) and the group velocity (3,100 m/s), the estimated distance is approximately $3100 * 2.5 * 10^{-4} = 77.5$ cm, which matches with the distance between sensors shown in Figure 2.

Figure 6 shows the actual values measured by sensor 2 (solid lines) and the predicted ouput by using model in (4) and sensor 1 as input. Since
the predicted output 100 steps ahead follows closely the harmonic behavior of the ultrasound waves measured by sensor 2, the model is valid for condition monitoring. Note that significant deviations between the predicted output and the actual values may be consequence of a fault.

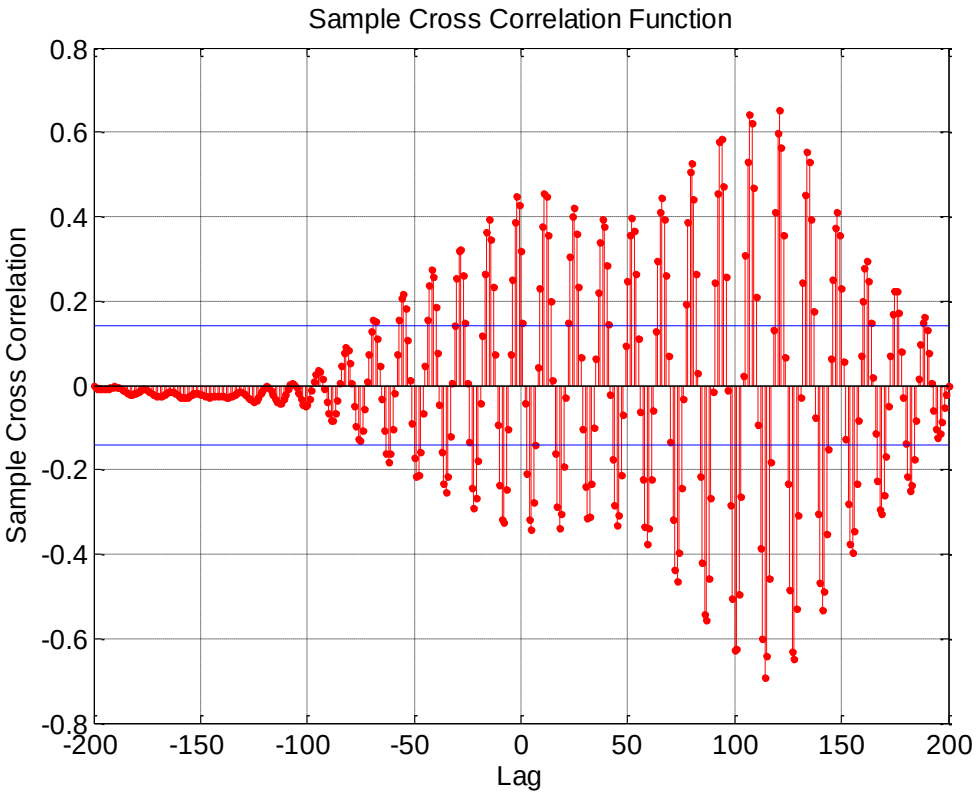

Figure 5. Cross-correlation graph between sensor 1 and sensor 2.

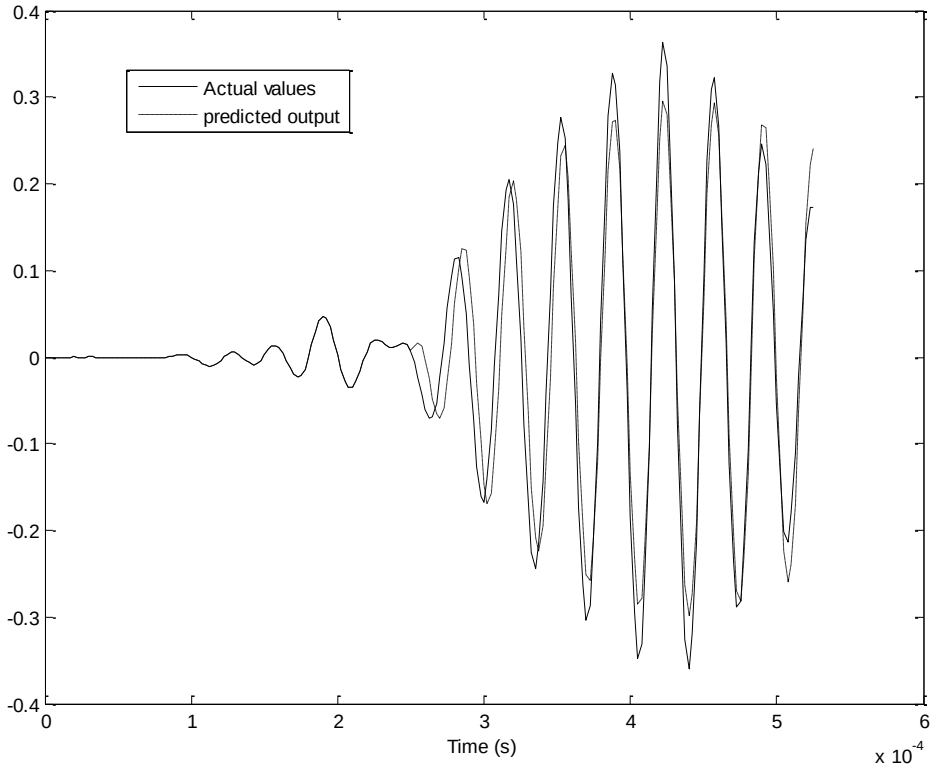

Figure 6. Actual values and predicted output with 100 steps ahead.

5. Conclusions

The development of condition monitoring techniques together with the use of advanced signal processing approaches to reduce the failure rate of PTRs is of paramount importance to increase the reliability, availability and investing returns in the generation of electricity by means of solar energy. This work reports a novel methodology to control the condition of the PTR steel part by means of ultrasounds and digital signal processing. Particularly, a methodology to identify models capable of predicting the fault-free output sensor signals has been proposed. In that sense, significant discrepancies between the predicted output and the actual measurements can work as an alarm signal to activate maintenance operations. Case studies based on laboratory experiments have shown promising results.

Further research might address the following issues: i) implementation of the proposed methodology for serially connected PTRs; ii) Categorization of different faults depending on the predicted output error pattern in conjunction with the incorporation of other exogenous variables as, for example, steel temperature; and iii) the use of different sensors/actuators to enhance the signal to noise ratio yielded by the MFCs.

Acknowledgements

This work has been supported by the EU project INTERSOLAR (Ref.: FP7-SME-2013-605028) and the MINECO project WindSeaEnergy (Ref.: IPT-2012-0563-120000).

References

1. D Dai, Q He, 'Structure damage localization with ultrasonic guided waves based on a time–frequency method', Signal Processing, Vol 96, pp 21-28, 2014.
2. X Wang, P W Tse, C K Mechefske, M Hua, 'Experimental investigation of reflection in guided wave-based inspection for characterization of pipeline defects', NDT&E International, Vol 43, pp 365–374, 2010.
3. L Sargent, N.R.E. Laboratory, Executive summary. 'Assessment of parabolic trough and power tower solar technology cost and performance forecasts', National Renewable Energy Laboratory, 2003.
4. C Kutscher, M Mehos, C Turchi, G Glatzmaier, 'Line-focus solar power plant cost reduction plan', Contract 2010;303:275–3000.
5. G E P Box, G M Jenkins, G C Reinsel, 'Time series analysis: forecasting and control' 4th edition, John Wiley & Sons, 2008.
6. Y Chen, 'Acoustical transmission line model for ultrasonic transducers for wide-bandwidth application', Acta Mechanica Solida Sinica, Vol 23, No 2, pp 124-134, 2010.
7. A Light-Marquez, A Sobin, G Park, K Farinholt, 'Structural damage identification in wind turbine blades using piezoelectric active sensing', Structural Dynamics and Renewable Energy, Vol 1, pp 55-65, 2011.
8. F P García, A M Tobias, J M Pinar,M Papaelias, 'Condition monitoring of wind turbines: Techniques and methods', Renewable Energy, Vol 46, pp 169-178, 2012.

9. F P García, D J Pedregal, C Roberts, ‘Time series methods applied to failure prediction and detection’, Reliability Engineering & System Safety, Vol 95, No 6, pp 698-703, 2010.
10. D J Pedregal, F P Garcia, C Roberts, ‘An algorithmic approach for maintenance management based on advanced state space systems and harmonic regressions’, Annals of Operations Research, Vol 166, No 1, pp 109-124, 2010.
11. L Ljung, ‘System identification, theory for the user. Second ed’, Upper Saddle River, NJ: PTR Prentice Hall, 2010.
12. Gómez Muñoz, C.Q.; García Márquez, F.P.; Trapero Arenas, J.R. In *Experimental platform design to monitor defects in wind turbine blades based on ultrasound technology*, The Energy and Environment Knowledge Week Congress, Toledo, Spain, 20/10/2013, 2013; Toledo, Spain.
13. H Akaike, ‘A new look at the statistical model identification’, IEEE Transactions on Automatic Control, Vol 19, No 6, pp 716-723, December 1974.
14. L Ljung, ‘System identification toolbox for use with Matlab (8th ed.)’, Natick, MA: The MathWorks, Inc., Version 8, 2012.
15. Gomez Munoz, C. Q., et al. "A novel approach to fault detection and diagnosis on wind turbines." *GLOBAL NEST JOURNAL* 16.6 (2014): 1029-1037.